Sulfate Radical-Induced Destruction of Emerging Contaminants Using Traces of Cobalt Ions as Catalysts

Yong Feng[1,2], Guang-Guo Ying[1,2], Zequn Yang[3], Kaimin Shih[3,*], Hailong Li[4], Deli Wu[5]

[1]SCNU Environmental Research Institute, Guangdong Provincial Key Laboratory of Chemical Pollution and Environmental Safety & MOE Key Laboratory of Theoretical Chemistry of Environment, South China Normal University, Guangzhou 510006, China

[2]School of Environment, South China Normal University, University Town, Guangzhou 510006, China

[3]Department of Civil Engineering, The University of Hong Kong, Pokfulam, Hong Kong, China

[4]School of Energy Science and Engineering, Central South University, Changsha 410083, China

[5]State Key Laboratory of Pollution Control and Resources Reuse, School of Environmental Science & Engineering, Tongji University, Shanghai 200092, China

Submitted to Chemosphere

Contacts:

Dr. Yong Feng (fengy@scnu.edu.cn)

Prof. Kaimin Shih (kshih@hku.hk)

***Corresponding author:**

Professor Kaimin Shih

Phone: +852-2859-1973

Fax: +852-2559-5337

E-mail: kshih@hku.hk

WORD COUNTs:

Text about 4735 words (Title + Abstract + Keywords + Manuscript body + Figure Captions + Acknowledgements) + 6 Figures = 6535 words

ABSTRACT

Cobalt is part of vitamin B12, which is essential to maintain human health, and trace levels of cobalt ions are ubiquitous in water and soil environments. In this study, the destruction of 1,4-dioxane (1,4-D) by peroxymonosulfate (PMS) under the catalysis of trace levels of Co^{2+} was investigated under buffered conditions. The results showed that near 100% removal of 1,4-D was achieved after reaction for 6 and 10 min with 50 and 25 μg/L Co^{2+}, respectively, in the presence of 5 mM phosphate ions. Mechanism studies revealed that radicals mediated the destruction of 1,4-D and sulfate radicals were the primary reactive species. The traces of Co^{2+} had the greatest reactivity for the catalysis of PMS in neutral environments (pH 7.0). However, pH 5.5 was observed to be the best condition for 1,4-D destruction, which was probably caused by the involvement of phosphate radicals. Common water components including chloride ions and bicarbonate ions were observed to have promoting and inhibiting effects, respectively, on the removal of 1,4-D. To further demonstrate the potential of Co^{2+}-PMS in practical applications, we explored the simultaneous degradation of 20 antibiotics using trace levels of Co^{2+}. The results showed that all the investigated antibiotics, except for lomefloxacin, could be efficiently degraded by Co^{2+}-PMS with removal rates of greater than 97%. The findings from this study demonstrate the promise of using trace levels of cobalt for environmental remediation applications, even when high concentrations of phosphate ions are co-present.

Keywords: 1,4-Dioxane; Antibiotics; Sulfate radicals; Degradation; Persulfate; Emerging contaminants

1. Introduction

1,4-Dioxane (1,4-D), a cyclic compound, is widely employed as an organic solvent in many industrial products. It is also commonly used to stabilize chlorinated solvents, particularly 1,1,1-trichloroethane, and is generated as a by-product in a wide range of consumer products (Mohr et al., 2010; Milavec et al., 2019). Due to the improper treatment of industrial wastes and organic solvents, leakage of 1,4-D into the environment has been documented (Mohr et al., 2010). 1,4-D is resistant to microbial treatment and has a very low soil sorption partition coefficient, which renders itself highly mobile in environmental matrices (Adamson et al., 2015). 1,4-D is miscible in water and has a low octanol–water partition coefficient (K_{ow}, $10^{0.27}$) and low vapor pressure (37 mmHg, 25 ºC), which makes itself difficult to be removed by conventional physical purification technologies, such as adsorption and air stripping (Sekar and DiChristina, 2014). In addition, traditional oxidants having a standard reduction potential of lower than 2.0 V are generally considered ineffective for the treatment of 1,4-D (Eberle et al., 2016). Although this substance has been recognized as a drinking water contaminant since 1978, a very recent study showed that the 1,4-D level in the drinking water of near 30 million people in the United States exceeds the health-based reference regulation (McElroy et al., 2019).

1,4-D has been classified as a carcinogen (Class 2B) and listed as an emerging contaminant by the U.S. EPA (Patton et al., 2016). Advanced oxidation processes (AOPs), particularly those relying on strong oxidizing radicals, such as hydroxyl radicals (·OH, E^0 (·OH/OH^-) = 1.8-2.7 V) and sulfate radicals ($SO_4^{\cdot-}$, E^0 ($SO_4^{\cdot-}/SO_4^{2-}$) = 2.5-3.1 V) (Buxton et al., 1988) (Neta et al., 1988), are compelling technologies for the treatment of recalcitrant contaminants and have been investigated to degrade 1,4-D. To generate ·OH for 1,4-D degradation, sonication (Son et al., 2006), Fenton reagents (Merayo et al., 2014), photocatalysis (Barndõk et al., 2016), and UV-assisted Fenton-like reactions (Patton et al., 2018) have been studied. Although ·OH is

highly reactive toward 1,4-D [(1.1-2.4) × 10^9 M^{-1} s^{-1})] (Adams et al., 1994), the application of ·OH-based AOPs in practical applications suffers from known scavenging problems due to the ubiquitous presence of radical scavengers (Hodges et al., 2018). Compared with ·OH ($t_{1/2}$ = 10^{-3} μs), $SO_4^{\cdot-}$ is more selective and has a significantly longer lifetime ($t_{1/2}$ = 30-40 μs). However, the later reactive species is significantly less investigated for 1,4-D removal (Cashman et al., 2019). The generation of $SO_4^{\cdot-}$ usually depends on the activation of either peroxydisulfate (PDS) or peroxymonosulfate (PMS) (Wang et al., 2014). Among the persulfate technologies reported for 1,4-D degradation, iron is the most commonly used material. Different forms of iron, such as Fe^{2+} (Zhao et al., 2014), zero-valent iron (Pang et al., 2019), iron oxides (Zhong et al., 2015), and iron minerals (Feng et al., 2018a), have been tested. Although decent performance was achieved, iron does not demonstrate true catalytic activity in these studies; the regeneration of ferrous iron is thermodynamically unfavourable and iron sludge is accumulated after neutralization (Hou et al., 2017).

$$Co^{2+} + HSO_5^- \rightarrow Co^{3+} + SO_4^{\cdot-} + OH^- \quad (1)$$

$$Co^{3+} + HSO_5^- \rightarrow Co^{2+} + SO_5^{\cdot-} + H^+ \quad (2)$$

Since its first-time application in pollutant removal (Anipsitakis and Dionysiou, 2003), the combination of PMS with Co^{2+} has been known for its powerful oxidizing capability. A similar performance could be achieved between the combinations of Co^{2+}-PMS and Fe^{2+}-H_2O_2 even if the concentration of Co^{2+} is 100 times lower than that of the Fe^{2+} (Bandala et al., 2007). This is not only because of the efficient activation of PMS by Co^{2+} to generate $SO_4^{\cdot-}$ (Eq. 1), but also because of the thermodynamic feasible reduction of Co^{3+} [E^0 (Co^{3+}/Co^{2+} = 1.92 V)] by PMS (Eq. 2) [$E^0(HSO_5^-/SO_4^{2-}$ = 1.75 V)] (Anipsitakis and Dionysiou, 2004). In addition, aqueous Co^{2+} ions are stable under aerobic conditions; the oxidation of Co^{2+} by dissolved molecular oxygen is extremely slow ($10^{-20.8}$ M^{-1} s^{-1}) (Rosso and Morgan, 2002). Although Co^{2+} can serve

as a real catalyst, its remanence in water solutions after treatment is a concern because of the potential toxicity of elevated levels of cobalt ions, which greatly limits its practical application. To this end, various solid Co-containing activators, such as cobalt oxides (Pang et al., 2020), cobalt bimetallic oxides (Ren et al., 2015), and Co-doped carbonaceous materials (Li et al., 2016), have been prepared and tested for PMS activation. However, trace levels of cobalt ions are still leached out even from stable Co-doped carbonaceous materials. For example, around 230 μg/L of cobalt ions were leached out from a highly efficient cobalt-graphene material (Li et al., 2018b). As the leaching seems inevitable, the purpose of this study was to examine the oxidative capability of PMS under the catalysis of trace levels of Co^{2+} ($\leq$ 50 μg/L) with 1,4-D and antibiotics as the target emerging contaminants. Antibiotics are widely used and frequently detected in the environments (Zhang et al., 2015), which is a great health concern. The concentration of Co^{2+} investigated in this study is lower than the level of Co^{2+} (usually greater than 100 μg/L) used to homogeneously catalyse PMS in literatures (Chen et al., 2019) and is comparable with the actual cobalt concentrations in various environmental matrices, particularly in soils and sediments (Collins and Kinsela, 2010; Izah et al., 2016).

2. **Experimental section**

2.1 Chemicals

PMS (Oxone ($2KHSO_5 \cdot KHSO_4 \cdot K_2SO_4$)), anhydrous 1,4-D (99.8%), sodium bicarbonate (99.5-100.5%), sodium thiosulfate ($\geqslant$ 99%), nitrobenzene (99%), and sodium chloride ($\geqslant$99.8%) were supplied by Sigma–Aldrich (St. Louis, MO, USA). *tert*-Butanol (99.5%) and 2,4-dinitrophenylhydrazine (98%) were obtained from Aladdin Corp. (Shanghai, China). Potassium iodide (99.8%) and sulfuric acid (98%) were purchased from BDH Chemicals (Poole, UK). Cobalt(II) nitrate hexahydrate (99%) and liquid chromatography (LC)-mass spectrometry (MS)–grade acetonitrile (methanol) were obtained from Merck Corp. (Darmstadt,

Germany). Twenty antibiotics with high purity (Table S1) were supplied by Dr. Ehrenstorfer GmbH (Germany).

2.2 Catalytic and degradation experiments

All the catalytic destruction reactions were conducted in 200-mL glass reactors at ambient temperature (25 ± 1 ˚C). The stock solutions of PMS (0.5 M), Co^{2+} (0.1 M), and 1,4-D (10 g/L) were prepared in advance by dissolving desired doses of Oxone, $Co(NO_3)_2$ powders, and anhydrous 1,4-D, respectively, in ultrapure water. Typically, ultrapure water (100 mL) was transferred to the reactor, followed by the addition of 1,4-D, PMS, and phosphate buffer. The pH value of the resulting solution was adjusted when necessary using diluted NaOH and H_2SO_4 solutions. To initiate catalytic and destruction reactions, Co^{2+} ($Co(NO_3)_2$ solution) was then added to the system. Liquid samples (1 mL) were collected using a pipette, transferred to LC auto-sampler vials (2 mL), and quenched immediately using excess sodium thiosulfate. The resulting samples were analysed within 30 min.

During the study of antibiotics, a stock solution containing 20 antibiotics (2 mg/L for each antibiotic) was prepared by dissolving desired amounts of chemical powders in LC-MS–grade methanol. To investigate their degradation by Co^{2+}-PMS, the antibiotic stock solution was then dried under nitrogen flow and redissolved in ultrapure water to achieve a target concentration of 50 μg/L for each compound. Before the analysis, the samples withdrawn were diluted with LC-MS–grade methanol and ultrapure water for 50 times (the diluted samples contained 50% of methanol (v/v)). Other steps were the same as that for the catalytic removal of 1,4-D.

2.3 Analysis of chemicals

1,4-D was measured using an Agilent 1260 Infinity II high-performance LC (HPLC) system equipped with a diode array detector (DAD) and an auto-sampler. A ZORBAX Eclipse XDB-C18 column (4.6 × 150 mm, 5 μm) was used for the separation. HPLC-grade acetonitrile and ultrapure water (10:90, v/v) were used as the mobile phase with a flow rate of 1 mL/min at a column temperature of 30 ºC. The DAD wavelength was set at 190 nm. The retention time of 1,4-D was around 2.4 min and the detection limit of 1,4-D was lower than 0.2 mg/L. PMS was quantified spectrometrically using an iodometric approach (Liang et al., 2008). The total organic carbon (TOC) was quantified using a TOC analyser (Shimadzu TOC-L series) via the combustion catalytic oxidation approach. Formaldehyde (HCHO) was quantified after reaction with 2,4-dinitrophenylhydrazine, details of which can be found in our previous publication (Feng et al., 2017a).

Twenty antibiotics were measured using an Acquity ultra-performance LC (UPLC) I-Class system coupled to a Xevo TQ-S triple quadrupole mass spectrometer (Waters Corp. Milford, MA, USA) with electrospray ionization under a positive ionization mode (UPLC-(ESI^+)-MS/MS). The separation was conducted on an Acquity UPLC BEH C18 column (2.1 mm × 50 mm, 1.7 μm). The quantification was carried out in multiple-reaction monitoring (MRM) modes. Detailed MRM transitions and the retention time of antibiotics are listed in Table S1. The injection volume of each sample was 2 μL, and the column temperature was fixed at 40 °C. The mobile phases consisted of ultrapure water (0.1% (v/v) formic acid, A) and methanol (B). The gradient program of the mobile phase is listed in Table S2. Details of MS parameters include a source temperature of 150 °C, a desolvation temperature of 500 °C, desolvation gas flow of 1, 000 L/h, and cone gas flow of 150 L/h. The quantification of limit for each antibiotic was lower than 20 ng/L, and calibration curves were established with a series of concentrations in the range of 20 to 1, 000 ng/L.

3. Results and discussion

3.1 Catalytic destruction of 1,4-D

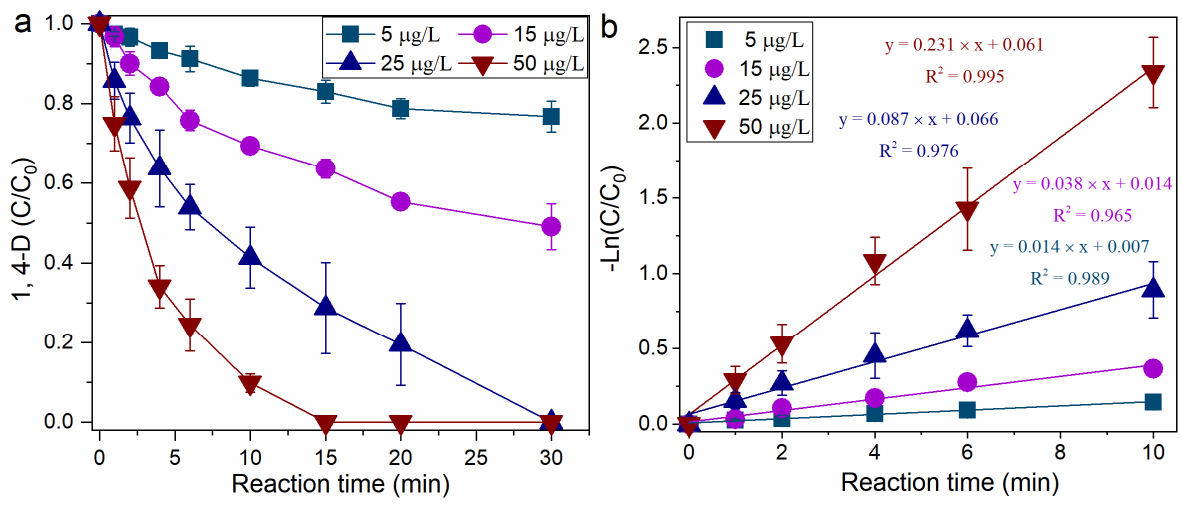

Figure 1. (a) Destruction of 1,4-D by PMS under the catalysis of different levels of Co^{2+} and (b) the corresponding pseudo–first-order rate constants (slopes). Experimental conditions: [PMS] = 2 mM, [1,4-D] = 5 mg/L, and 5 mM phosphate buffer at pH 7.0.

PMS alone had no obvious capability to degrade 1,4-D (Feng et al., 2017a). The destruction of 1,4-D in Co^{2+}-PMS oxidation was investigated in the presence of different doses of Co^{2+}. As shown in Fig. 1a, near 100% destruction of 1,4-D was achieved after reaction for 15 min with 50 μg/L Co^{2+} and 2 mM PMS. When the concentration of Co^{2+} was reduced to 25 μg/L, similar destruction performance was observed after reaction for 30 min. These phenomena suggest that trace levels of Co^{2+} have great reactivity for 1,4-D destruction via the catalysis of PMS. The destruction of 1,4-D by Co^{2+}-PMS was well modelled by the pseudo–first-order law (Fig. 1b). By plotting $-\ln(C/C_0)$ versus reaction time (min), the pseudo–first-order rate constants with 5, 15, 25 and 50 μg/L of Co^{2+} were calculated to be 0.014, 0.038, 0.087, and 0.231 min^{-1} (Fig. 1b), respectively.

3.2 Effect of pH on Co^{2+}-PMS

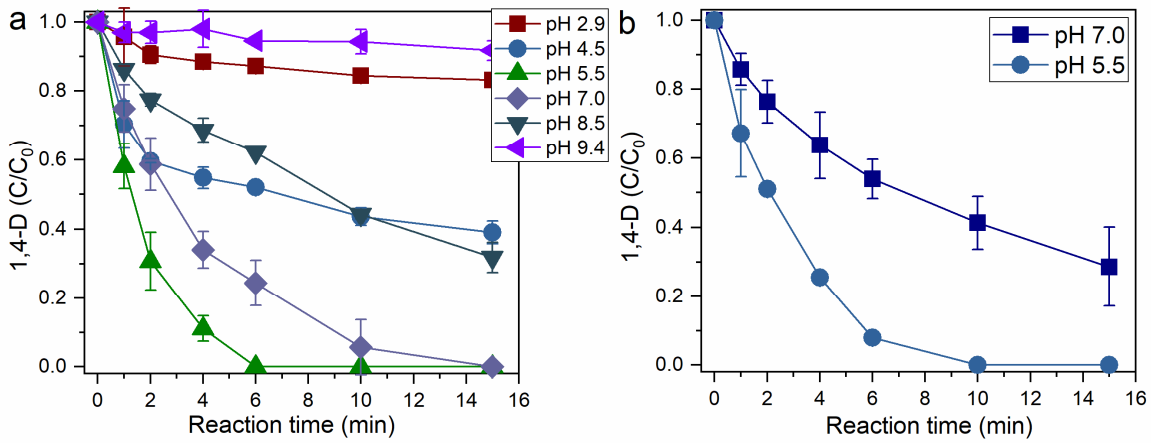

Figure 2. (a) Reactivity of Co^{2+}-PMS under different pH values and (b) destruction of 1,4-D by PMS under the catalysis of 25 μg/L Co^{2+}. Experimental conditions: [PMS] = 2 mM, [Co^{2+}] = (a) 50 and (b) 25 μg/L, [1,4-D] = 5 mg/L, 5 mM acetate buffer (pH 4.5), 5 mM phosphate buffer (pH 5.5, 7.0, 8.5), and 5 mM boric buffer (pH 9.4).

Solution pH value is a key parameter in environmental redox chemistry. To fully demonstrate the oxidative capability of Co^{2+}-PMS, we studied the destruction of 1,4-D under different pH values. The results showed that both strongly acidic and alkaline environments were detrimental to the destruction; overall removal rates of only around 13% and 9% were achieved at the pH value of 2.9 and 9.4, respectively (Fig. 2a). The combination of Co^{2+} with PMS had the best reactivity at pH 5.5; near 100% destruction of 1,4-D was observed after reaction for only 6 min under the catalysis of 50 μg/L Co^{2+}. When 25 μg/L Co^{2+} was used, the reaction time for completely removing 1,4-D at pH 5.5 was extended to 10 min (Fig. 2b). To reveal the mineralization of 1,4-D, the removal of TOC was studied. The results demonstrated that only around 14.5% of the TOC was removed after reaction for 15 min (Fig. S2). This removal rate was significantly lower than the destruction rate of 1,4-D.

The $pK_{a,2}$ of PMS is around 9.4, and thus PMS primarily existed as HSO_5^- when the pH value ranged from 2.9 to 8.5. 1,4-D has a pK_a value of -2.92 (Perrin, 1972), which means that 1,4-D

existed as neutral molecules under the investigated pH conditions. The low reactivity at pH 2.9 could be related to the stabilization effect of excess H^+ ions on the decomposition of PMS (Zhang et al., 2013). In the pH range of 5.5 to 8.5, the degradation obviously slowed down, which was probably caused by the variation in the speciation of cobalt ions.

3.3 Degradation mechanism and active species

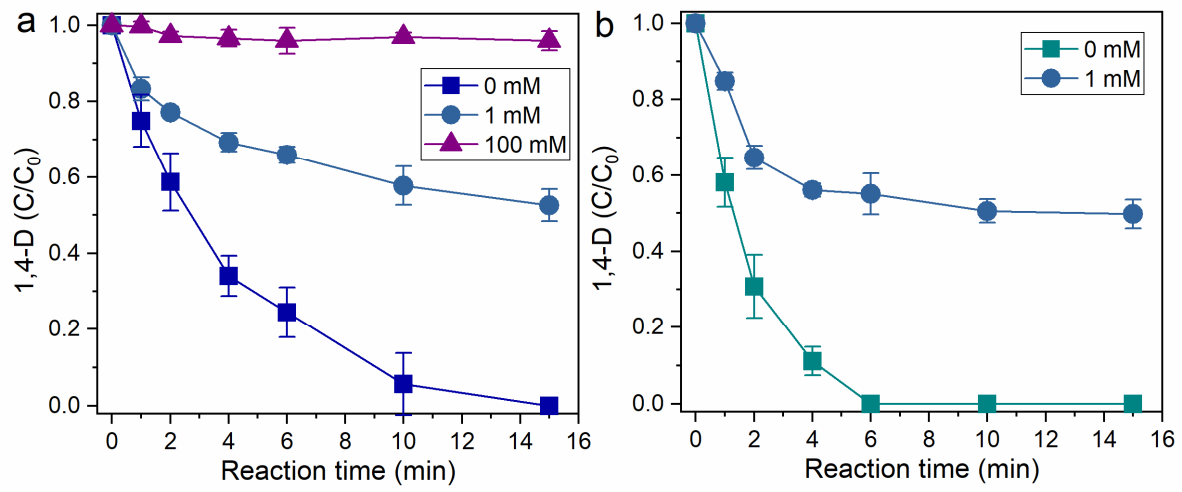

Figure 3. Influence of methanol on the destruction of 1,4-D in Co^{2+}-PMS oxidation at pH (a) 7.0 and (b) 5.5. Experimental conditions: [PMS] = 2 mM, [Co^{2+}] = 50 μg/L, [1,4-D] = 5 mg/L, and 5 mM phosphate buffer.

To examine the removal mechanism, the role of radicals in the degradation was investigated by conducting scavenging experiments. Methanol reacts rapidly with both $SO_4^{\cdot-}$ (2.5 ± 0.4) × 10^7 M^{-1} s^{-1}) (Ross and Neta, 1979) and ·OH (9.7 × 10^8 M^{-1} s^{-1}) (Buxton et al., 1988), and thus this compound was used as a scavenger. The results revealed that the overall destruction rate of 1,4-D decreased from around 100% to 47% and 50% at pH 7.0 (Fig. 3a) and pH 5.5 (Fig. 3b), respectively, in the presence of 1 mM methanol. When methanol was further increased to 100 mM, near complete inhibition of the degradation was observed (Fig. 3a). In addition to radicals, singlet oxygen ($^1O_2$) (Zhou et al., 2015), superoxide radicals ($O_2^{\cdot-}$), and peroxymonosulfate radical ($SO_5^{\cdot-}$) were proposed to be generated as reactive species during the

activated decomposition of PMS. However, $^1O_2$-mediated oxidation cannot be quenched by methanol (Zhou et al., 2015), and therefore, the involvement of $^1O_2$ can be excluded. Meanwhile, the contribution of $O_2^{\cdot-}$ ($E^0(O_2^{\cdot-}/O_2)$ = -0.33 V) (Wardman, 1989) and $SO_5^{\cdot-}$ ($E^0(SO_5^{\cdot-}/HSO_5^-)$ = 1.1 V) (Neta et al., 1988) to the degradation of organic contaminants in homogeneous systems is usually negligible due to their low oxidation potential and rapid transformation (Qin et al., 2018). Therefore, it can be concluded that radicals ($SO_4^{\cdot-}$, ·OH) were key to the destruction of 1,4-D, which confirms the findings by Cashman et al. (Cashman et al., 2019).

tert-Butanol, without an α-hydrogen in its structure, is usually the alcohol used to reveal the contribution of $SO_4^{\cdot-}$. However, our experiments showed that *tert*-butanol had significant interference in the analysis of 1,4-D, and therefore, nitrobenzene was instead used to further differentiate the produced radicals. In our precious work, nitrobenzene has shown effectiveness in the differentiation of $SO_4^{\cdot-}$ and ·OH (Feng et al., 2017b); nitrobenzene can be rapidly oxidized by ·OH (3.9×10^9 M^{-1} s^{-1}), but is not very reactive toward $SO_4^{\cdot-}$ ($< 10^6$ M^{-1} s^{-1}) (Neta et al., 1977; Buxton et al., 1988). When Co^{2+} was absent, only 3.2% of the nitrobenzene was removed by PMS alone (Fig. S1). When 50 μg/L of Co^{2+} is co-present with PMS, 27.1% of the nitrobenzene (0.1 mM) was degraded (Fig. S1). Under identical conditions, near 100% of the 1,4-D (5.68 μM) was removed by Co^{2+}-PMS (Fig. 3a). For the oxidation of 1,4-D and nitrobenzene by radicals, $SO_4^{\cdot-}$ has a relatively greater rate constant with 1,4-D [$(4.1\text{-}5.7) \times 10^7$ M^{-1} s^{-1}] (Huie et al., 1991) and ·OH is relatively more reactive toward nitrobenzene (3.9×10^9 M^{-1} s^{-1}) (Buxton et al., 1988). Therefore, the greater degradation of 1,4-D than nitrobenzene reveals that $SO_4^{\cdot-}$ was the dominant radicals produced in Co^{2+}-PMS oxidation, which is in line with Anipsitakis and Dionysiou's results (Anipsitakis and Dionysiou, 2003). However, the

obvious degradation of nitrobenzene by Co^{2+}-PMS suggests that ·OH was also involved, which was probably due to the interaction of $SO_4^{\cdot-}$ with OH^-. Meanwhile, the overall removal percentage of TOC was less than 15% (Fig. S2), which can be explained by the dominance of $SO_4^{\cdot-}$. Small-molecular carboxylic acids and esters were the major products of 1,4-D oxidation by $SO_4^{\cdot-}$ and ·OH (Feng et al., 2017a), and in our previous work we have demonstrated that the degradation of ethers, such as ethylene glycol diformate, is much more difficult than that of 1,4-D in $SO_4^{\cdot-}$-mediated oxidation (Feng et al., 2017a). In addition, $SO_4^{\cdot-}$ is also relatively low reactive toward common carboxylic acids, such as acetic acid ($4.3 \times 10^6\ M^{-1}\ s^{-1}$) (Huie and Clifton, 1990).

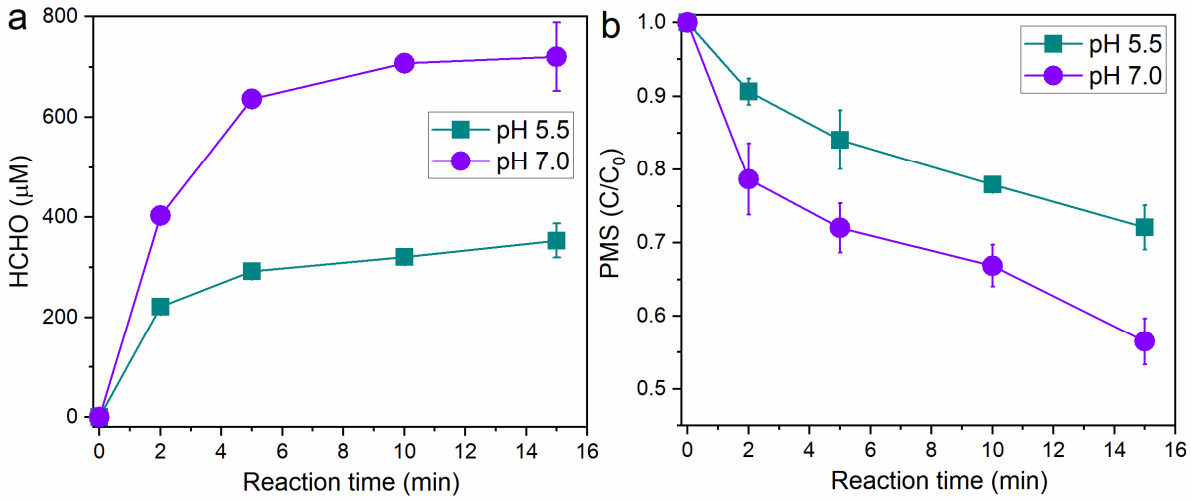

Figure 4. (a) Generation of HCHO from methanol oxidation by Co^{2+}-PMS under different pH values and (b) the corresponding decomposition of PMS. Conditions: [PMS] = 2 mM, [Co^{2+}] = 50 μg/L, [methanol] = 0.25 M, and 5 mM phosphate buffer.

To further examine the catalysis of PMS by Co^{2+}, we quantified the produced reactive species using excess methanol as a substrate. Under the attack of radicals, methanol is oxidized to HCHO (Feng et al., 2017a). The results showed that HCHO was generated at both pH values, but the overall HCHO produced at pH 7.0 (720.1 μM) was much greater than that produced at pH 5.5 (349.5 μM, Fig. 4). Correspondingly, more rapid decomposition of PMS occurred at pH 7.0. According to Eq. 3, the stoichiometric efficiencies at pH 7.0 and 5.5 were calculated

to be around 83% and 63%, respectively. The generation of one mole of $SO_4^{\cdot-}$ and regeneration of Co^{2+} requires two moles of PMS (Eqs. 1 and 2), the high stoichiometric efficiencies recorded in this study probably suggest the involvement of other species, such as $CH_2OH\cdot$, in the reduction of Co^{3+}. In addition, high-valent metal complexes are proposed to be generated as one of the oxidizing species during the interaction of some transition metals with PMS (Feng et al., 2018b; Li et al., 2018a), and thus the possible formation of Co^{IV}=O in Co^{2+}-PMS oxidation needs to be explored in future studies (Brunschwig et al., 1983; Pfaff et al., 2011).

$$\text{Stoichiometric efficiency} = \frac{\Delta[\text{HCHO}]}{\Delta[\text{PMS}]} \quad (3)$$

The much greater generation of HCHO at pH 7.0 seems contraire with the destruction of 1,4-D observed in Fig. 2. As a relatively high level of phosphate buffer (5 mM, [phosphate buffer]/[1,4-D] = 88) was present, this discrepancy probably resulted from the scavenging effect of phosphate ions. The second-order rate constant between $SO_4^{\cdot-}$ and HPO_4^{2-} is (1.2 ± 0.3) × 10^6 M^{-1} s^{-1}, and the rate constant of $SO_4^{\cdot-}$ with 1,4-D is (4.1-5.7) × 10^7 M^{-1} s^{-1}. Under the attack of $SO_4^{\cdot-}$, phosphate ions were transferred to phosphate radicals. According to the fast acid-base equilibria shown in Eq. 4 (Cencione et al., 1998), the primary phosphate radicals at pH 5.5 and pH 7.0 were $H_2PO_4^{\cdot}$ and $HPO_4^{\cdot}$, respectively. The destruction of 1,4-D by $SO_4^{\cdot-}$ mainly proceeded via hydrogen abstraction (Huie et al., 1991). $H_2PO_4^{\cdot}$ may have similar abstraction reactivity to $SO_4^{\cdot-}$, but the reactivity of $HPO_4^{\cdot}$ and $PO_4^{\cdot 2-}$ are much weaker (Maruthamuthu and Neta, 1978). For example, the rate constants for the oxidation of α, α, α-trifluorotoluene by $SO_4^{\cdot-}$, $H_2PO_4^{\cdot}$, $HPO_4^{\cdot}$, and $PO_4^{\cdot 2-}$ were (2 ± 1) × 10^7, (3.5 ± 0.5) × 10^7, (2.7 ± 0.5) × 10^6, and (9 ± 1) × 10^5 M^{-1} s^{-1} (Rosso et al., 1999), respectively. When the pH value rose from 5.5 to 7.0, the produced primarily phosphate radicals shifted from $H_2PO_4^{\cdot}$ to $HPO_4^{\cdot}$, which led to a decrease in the reactivity of the reaction system. However, the generation of phosphate radicals could be ignored when a high level of methanol (0.25 M) was present.

Therefore, it can be concluded that the combination of Co^{2+} with PMS had the greatest reactivity at pH 7.0.

$$H_2PO_4^{\cdot} \overrightarrow{\overleftarrow{pK_a = 5.7}} HPO_4^{\cdot} \overrightarrow{\overleftarrow{pK_a = 8.9}} PO_4^{\cdot 2-} \quad (4)$$

3.4 Effects of chloride and bicarbonate ions

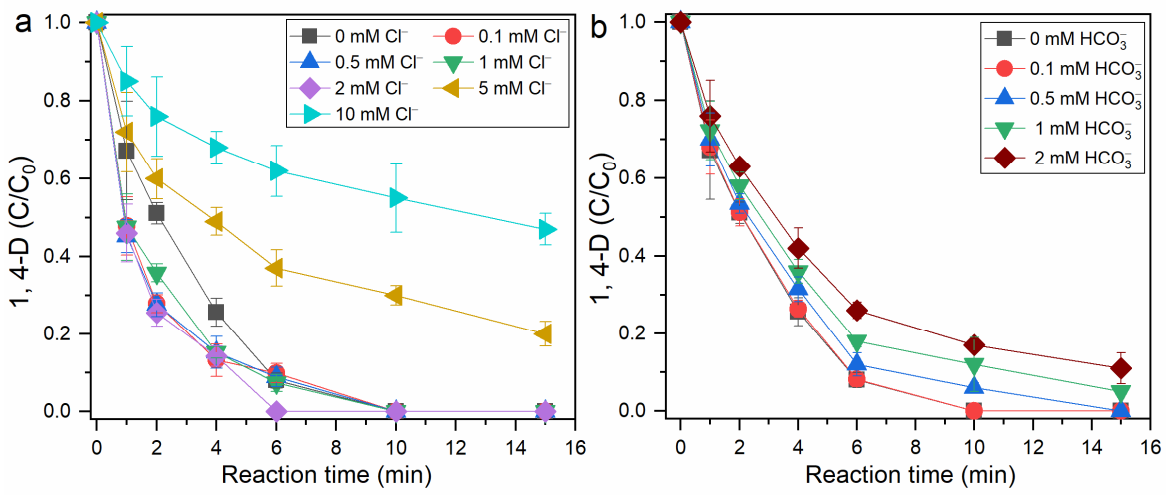

Figure 5. Effects of (a) Cl^- and (b) HCO_3^- on the destruction of 1,4-D in Co^{2+}-PMS oxidation. Experimental conditions: [PMS] = 2 mM, [Co^{2+}] = 25 μg/L, [1,4-D] = 5 mg/L, and 5 mM phosphate buffer (pH 5.5). The pH value of the 1,4-D solutions that contain phosphate buffer (5 mM), varied levels of bicarbonate, and PMS was adjusted to 5.5 before the spiking of Co^{2+} to initiate catalytic degradation.

Chloride ions (Cl^-) are ubiquitous in various water bodies and are common scavengers for radicals, particularly for $SO_4^{\cdot -}$. Excess Cl^- ions react rapidly with $SO_4^{\cdot -}$ (3.1×10^8 M^{-1} s^{-1}) to generate chloride radicals [$Cl_2^{\cdot -}$, $E^0(Cl_2^{\cdot -}/2Cl^-) = 2.09$ V] and $Cl_2^{\cdot -}$ is less reactive than $SO_4^{\cdot -}$ [$E^0(SO_4^{\cdot -}/SO_4^{2-}) = (2.5 - 3.1)$ V]. In previous publications, both promoting and inhibition effects of Cl^- on $SO_4^{\cdot -}$-mediated oxidation have been reported (Chan and Chu, 2009; Feng et al., 2018c). To demonstrate the capability of Co^{2+}-PMS for practical applications, the influence of Cl^- on the destruction of 1,4-D was studied. The results showed that Cl^- with concentrations in the range of 0.1 to 2 mM had no inhibitory effect on the degradation (Fig. 5a). Instead, a slight promoting effect, particularly in the presence of 2 mM Cl^-, was observed. As discussed

above, $H_2PO_4^{\cdot}$ probably contributed to the degradation. The slight promoting effect possibly resulted from the reduced generation of $H_2PO_4^{\cdot}$ and the involvement of $Cl_2^{\cdot-}$. When the concentration of Cl^- was further increased to 5 and 10 mM, significant inhibitory effects were observed, which is consistent with our previous studies (Feng et al., 2017a; Feng et al., 2018a). Although the active chlorine species (e.g., $Cl_2^{\cdot-}$ and HClO) generated in the presence of chloride ions are capable of oxidizing some organic contaminants and may even show promoting effects (Yuan et al., 2011; Huang et al., 2017; Sheng et al., 2018; Yang et al., 2018), these species are more selective than $SO_4^{\cdot-}$ and are relatively low reactive toward 1,4-D. $Cl_2^{\cdot-}$ oxidizes 1,4-D at a second-order rate constant of $(3.3 \pm 0.18) \times 10^6\ M^{-1}\ s^{-1}$ (Patton et al., 2016), and this value is significantly lower than the constant between $SO_4^{\cdot-}$ and 1,4-D [$(4.1\text{-}5.7) \times 10^7\ M^{-1}\ s^{-1}$].

In addition to Cl^-, HCO_3^- ions are usually expected to consume radicals significantly in natural water. Meanwhile, HCO_3^- reacts with $SO_4^{\cdot-}$ [$(4.6 \pm 0.5) \times 10^6\ M^{-1}\ s^{-1}$) (Shafirovich et al., 2001) to generate less oxidizing carbonate radicals ($CO_3^{\cdot-}$, $E^0 = (CO_3^{\cdot-}/CO_3^{2-})$ = 1.57 V) (Armstrong et al., 2013). Therefore, the influence of HCO_3^- on the destruction of 1,4-D was also studied. Results demonstrated that, in contrast to the promoting effect, the addition of HCO_3^- inhibited the destruction of 1,4-D (Fig. 5b). When HCO_3^- was in the range of 0.1 to 2 mM, the inhibitory extent was positively correlated with the concentration of HCO_3^-. These obvious scavenging effects could be explained by the consumption of $SO_4^{\cdot-}$ and the much weaker oxidative capability of $CO_3^{\cdot-}$. The levels of Cl^- and HCO_3^- studied in this study are compatible with their contents in groundwater and surface water (Yang et al., 2015).

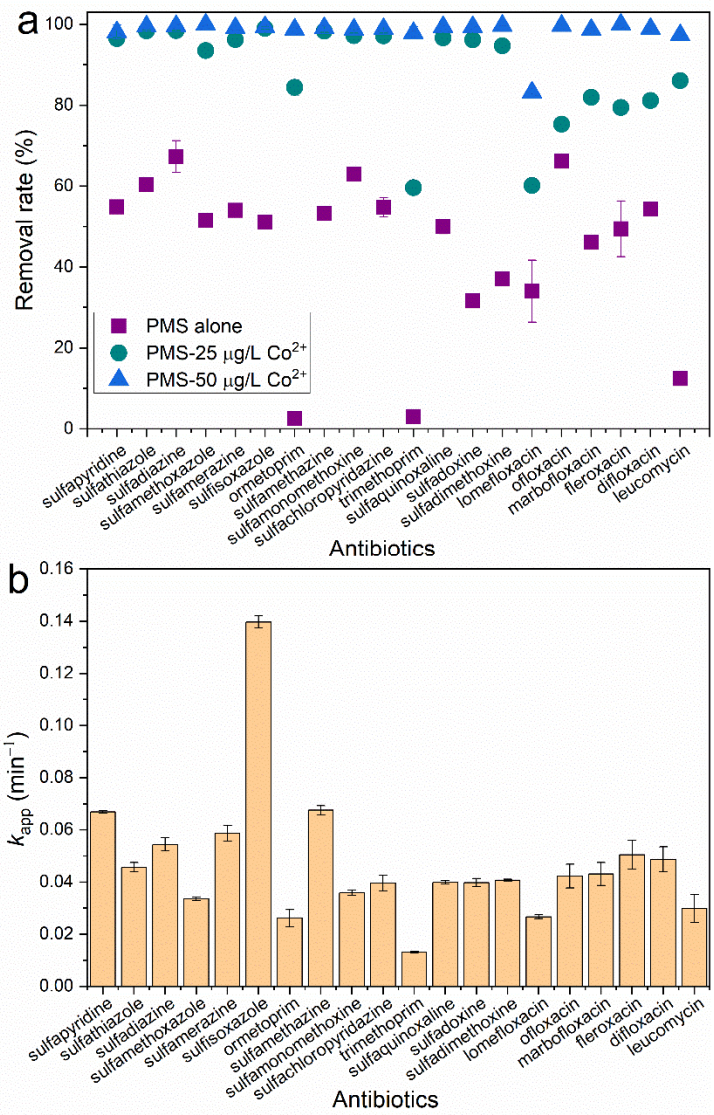

Figure 6. (a) Simultaneous removal of 20 antibiotics by Co^{2+}-PMS and (b) their corresponding pseudo–first-order rate constants. Experimental conditions: [PMS] = 1 mM, [each antibiotic] = 50 μg/L, and reaction time = (a) 60 min and (b) 30 min. The initial pH value of the solution containing 20 antibiotics was not adjusted after the addition of PMS.

One characteristic with the pollution of antibiotics is their relatively low concentrations and coexistence of various categories with different properties. To further demonstrate the practical applicability, we investigated the simultaneous degradation of 20 antibiotics by Co^{2+}-PMS. The antibiotics investigated here are widely used in China (Zhang et al., 2015). The results showed that most of the antibiotics could be degraded by unactivated PMS, although the removal rates (35 to 70%, Fig. 6a) are not satisfying. Antibiotics including ormetoprim, trimethoprim, and

leucomycin were relatively more resistant to PMS oxidation. When Co^{2+} ions were added as catalysts, the degradation of all the investigated antibiotics was significantly increased. The overall degradation rates of ormetoprim, trimethoprim, and leucomycin were increased from 2.5%, 3.1%, and 12.4% to 84.4%, 59.7%, and 86.0%, respectively, in the presence of 25 μg/L Co^{2+}. The degradation rates of all the antibiotics, except for lomefloxacin, were greater than 97% when the concentration of Co^{2+} further rose to 50 μg/L. Kinetic investigations demonstrated that the destruction of antibiotics followed pseudo–first-order kinetics at the beginning 30 min. The obtained pseudo–first-order constants reveal that sulfisoxazole and trimethoprim were the easiest and most difficult compounds, respectively, to be degraded by Co^{2+}-PMS (Fig. 6b).

4. Conclusions

Trace levels of Co^{2+} were used as catalysts for PMS decomposition to degrade 1,4-D. The combination of PMS with Co^{2+} had a wide effective pH range (4.5 to 8.5); the pH value is typically found in the terrestrial environment. On the basis of the experimental observations, some conclusions can be drawn as follows:

(1) PMS could not obviously oxidize 1,4-D, and therefore unactivated PMS is inefficient to degrade 1,4-D;

(2) Rapid destruction of 1,4-D was observed when PMS co-presented with trace levels of Co^{2+}; almost complete destruction was observed after reaction for only 6 min under the catalysis of 50 μg/L Co^{2+};

(3) Although trace levels of Co^{2+} could rapidly remove 1,4-D via catalysing PMS, their reactivity is quite limited during the mineralization;

(4) The destruction of 1,4-D was mediated by radicals, and $SO_4^{\cdot-}$ was the dominant reactive species;

(5) Although pH 5.5 was the optimum condition for 1,4-D degradation, the best pH condition for the activation of PMS by Co^{2+} was 7.0;

(6) Compared with the other antibiotics investigated, ormetoprim, trimethoprim, and leucomycin were relatively more difficult to be oxidized by unactivated PMS;

(7) Of the investigated antibiotics, lomefloxacin was the compound most difficult to be degraded by Co^{2+}-PMS. The overall degradation rates of all the other antibiotics were greater than 97%.

Acknowledgements

This study was funded by the Research Grants Council of Hong Kong (Projects 106180082, C7044-14G, and T21-711/16R) and the start-up fund from South China Normal University (Project 8S0597).

References

Adams, C.D., Scanlan, P.A., Secrist, N.D., 1994. Oxidation and biodegradability enhancement of 1,4-dioxane using hydrogen peroxide and ozone. Environ. Sci. Technol. 28, 1812-1818.

Adamson, D.T., Anderson, R.H., Mahendra, S., Newell, C.J., 2015. Evidence of 1,4-dioxane attenuation at groundwater sites contaminated with chlorinated solvents and 1,4-dioxane. Environ. Sci. Technol. 49, 6510-6518.

Anipsitakis, G.P., Dionysiou, D.D., 2003. Degradation of organic contaminants in water with sulfate radicals generated by the conjunction of peroxymonosulfate with cobalt. Environ. Sci. Technol. 37, 4790-4797.

Anipsitakis, G.P., Dionysiou, D.D., 2004. Radical generation by the interaction of transition metals with common oxidants. Environ. Sci. Technol. 38, 3705-3712.

Armstrong, D.A., Huie, R.E., Lymar, S., Koppenol, W.H., Merényi, G., Neta, P., Stanbury, D.M., Steenken, S., Wardman, P., 2013. Standard electrode potentials involving radicals in aqueous solution: inorganic radicals. BioInorganic Reaction Mechanisms 9, 59-61.

Bandala, E.R., Peláez, M.A., Dionysiou, D.D., Gelover, S., Garcia, J., Macías, D., 2007. Degradation of 2,4-dichlorophenoxyacetic acid (2,4-D) using cobalt-peroxymonosulfate in Fenton-like process. J. Photochem. Photobiol. A. Chem. 186, 357-363.

Barndõk, H., Hermosilla, D., Han, C., Dionysiou, D.D., Negro, C., Blanco, Á., 2016. Degradation of 1,4-dioxane from industrial wastewater by solar photocatalysis using immobilized NF-TiO_2 composite with monodisperse TiO_2 nanoparticles. Appl. Catal., B 180, 44-52.

Brunschwig, B.S., Chou, M.H., Creutz, C., Ghosh, P., Sutin, N., 1983. Mechanisms of water oxidation to oxygen: Cobalt(IV) as an intermediate in the aquocobalt(II)-catalyzed reaction. J. Am. Chem. Soc. 105, 4832-4833.

Buxton, G.V., Greenstock, C.L., Helman, W.P., Ross, A.B., 1988. Critical review of rate constants for reactions of hydrated electrons, hydrogen atoms and hydroxyl radicals ($\cdot OH/\cdot O^-$) in aqueous solution. J. Phys. Chem. Ref. Data 17, 513-886.

Cashman, M.A., Kirschenbaum, L., Holowachuk, J., Boving, T.B., 2019. Identification of hydroxyl and sulfate free radicals involved in the reaction of 1,4-dioxane with peroxone activated persulfate oxidant. J. Hazard. Mater. 380, 120875.

Cencione, S.S., Gonzalez, M.C., Mártire, D.O., 1998. Reactions of phosphate radicals with substituted benzenes. A structure–reactivity correlation study. J. Chem. Soc., Faraday Trans. 94, 2933-2937.

Chan, K., Chu, W., 2009. Degradation of atrazine by cobalt-mediated activation of peroxymonosulfate: Different cobalt counteranions in homogenous process and cobalt oxide catalysts in photolytic heterogeneous process. Water Res. 43, 2513-2521.

Chen, M., Zhu, L., Liu, S., Li, R., Wang, N., Tang, H., 2019. Efficient degradation of organic pollutants by low-level Co^{2+} catalyzed homogeneous activation of peroxymonosulfate. J. Hazard. Mater. 371, 456-462.

Collins, R.N., Kinsela, A.S., 2010. The aqueous phase speciation and chemistry of cobalt in terrestrial environments. Chemosphere 79, 763-771.

Eberle, D., Ball, R., Boving, T.B., 2016. Peroxone activated persulfate treatment of 1, 4-dioxane in the presence of chlorinated solvent co-contaminants. Chemosphere 144, 728-735.

Feng, Y., Lee, P.H., Wu, D., Shih, K., 2017a. Surface-bound sulfate radical-dominated degradation of 1,4-dioxane by alumina-supported palladium (Pd/Al_2O_3) catalyzed peroxymonosulfate. Water Res. 120, 12-21.

Feng, Y., Li, H.L., Lin, L., Kong, L.J., Li, X.Y., Wu, D.L., Zhao, H.Y., Shih, K., 2018a. Degradation of 1,4-dioxane via controlled generation of radicals by pyrite-activated oxidants: Synergistic effects, role of disulfides, and activation sites. Chem. Eng. J. 336, 416-426.

Feng, Y., Liao, C., Kong, L., Wu, D., Liu, Y., Lee, P.H., Shih, K., 2018b. Facile synthesis of highly reactive and stable Fe-doped g-C_3N_4 composites for peroxymonosulfate activation: A novel nonradical oxidation process. J. Hazard. Mater. 354, 63-71.

Feng, Y., Wu, D., Zhou, Y., Shih, K., 2017b. A metal-free method of generating sulfate radicals through direct interaction of hydroxylamine and peroxymonosulfate: Mechanisms, kinetics, and implications. Chem. Eng. J. 330, 906-913.

Feng, Y., Wu, D.L., Li, H.L., Bai, J.F., Hu, Y.B., Liao, C.Z., Li, X.Y., Shih, K., 2018c. Activation of persulfates using siderite as a source of ferrous ions: Sulfate radical production, stoichiometric efficiency, and implications. ACS Sustain. Chem. Eng. 6, 3624-3631.

Hodges, B.C., Cates, E.L., Kim, J.H., 2018. Challenges and prospects of advanced oxidation water treatment processes using catalytic nanomaterials. Nat. Nanotechnol. 13, 642.

Hou, X., Huang, X., Jia, F., Ai, Z., Zhao, J., Zhang, L., 2017. Hydroxylamine promoted goethite surface Fenton degradation of organic pollutants. Environ. Sci. Technol. 51, 5118-5126.

Huang, Y., Yang, F., Ai, L., Feng, M., Wang, C., Wang, Z., Liu, J., 2017. On the kinetics of organic pollutant degradation with Co^{2+}/peroxymonosulfate process: When ammonium meets chloride. Chemosphere 179, 331-336.

Huie, R.E., Clifton, C.L., 1990. Temperature dependence of the rate constants for reactions of the sulfate radical, SO_4^-, with anions. J. Phys. Chem. 94, 8561-8567.

Huie, R.E., Clifton, C.L., Kafafi, S.A., 1991. Rate constants for hydrogen abstraction reactions of the sulfate radical, SO_4^-: Experimental and theoretical results for cyclic ethers. J. Phys. Chem. 95, 9336-9340.

Izah, S.C., Chakrabarty, N., Srivastav, A.L., 2016. A review on heavy metal concentration in potable water sources in Nigeria: Human health effects and mitigating measures. Exposure and Health 8, 285-304.

Li, H., Shan, C., Pan, B., 2018a. Fe(III)-doped g-C_3N_4 mediated peroxymonosulfate activation for selective degradation of phenolic compounds via high-valent iron-oxo species. Environ. Sci. Technol. 52, 2197-2205.

Li, X., Huang, X., Xi, S., Miao, S., Ding, J., Cai, W., Liu, S., Yang, X., Yang, H., Gao, J., Wang, J., Huang, Y., Zhang, T., Liu, B., 2018b. Single cobalt atoms anchored on porous N-doped graphene with dual reaction sites for efficient Fenton-like catalysis. J. Am. Chem. Soc. 140, 12469-12475.

Li, X.N., Ao, Z.M., Liu, J.Y., Sun, H.Q., Rykov, A.I., Wang, J.H., 2016. Topotactic transformation of metal-organic frameworks to graphene-encapsulated transition-metal nitrides as efficient Fenton-like catalysts. ACS Nano 10, 11532-11540.

Liang, C., Huang, C., Mohanty, N., Kurakalva, R.M., 2008. A rapid spectrophotometric determination of persulfate anion in ISCO. Chemosphere 73, 1540-1543.

Maruthamuthu, P., Neta, P., 1978. Phosphate radicals. Spectra, acid-base equilibriums, and reactions with inorganic compounds. J. Phys. Chem. 82, 710-713.

McElroy, A.C., Hyman, M.R., Knappe, D.R.U., 2019. 1,4-Dioxane in drinking water: Emerging for 40 years and still unregulated. Current Opinion in Environmental Science & Health 7, 117-125.

Merayo, N., Hermosilla, D., Cortijo, L., Blanco, Á., 2014. Optimization of the Fenton treatment of 1,4-dioxane and on-line FTIR monitoring of the reaction. J. Hazard. Mater. 268, 102-109.

Milavec, J., Tick, G.R., Brusseau, M.L., Carroll, K.C., 2019. 1,4-Dioxane cosolvency impacts on trichloroethene dissolution and sorption. Environ. Pollut. 252, 777-783.

Mohr, T.K., Stickney, J.A., DiGuiseppi, W.H., 2010. Environmental investigation and remediation: 1,4-Dioxane and other solvent stabilizers. CRC Press.

Neta, P., Huie, R.E., Ross, A.B., 1988. Rate constants for reactions of inorganic radicals in aqueous solution. J. Phys. Chem. Ref. Data 17, 1027-1284.

Neta, P., Madhavan, V., Zemel, H., Fessenden, R.W., 1977. Rate constants and mechanism of reaction of sulfate radical anion with aromatic compounds. J. Am. Chem. Soc. 99, 163-164.

Pang, Y., Kong, L., Chen, D., Yuvaraja, G., Mehmood, S., 2020. Facilely synthesized cobalt doped hydroxyapatite as hydroxyl promoted peroxymonosulfate activator for degradation of Rhodamine B. J. Hazard. Mater. 384, 121447.

Pang, Y., Ruan, Y., Feng, Y., Diao, Z., Shih, K., Hou, L.a., Chen, D., Kong, L., 2019. Ultrasound assisted zero valent iron corrosion for peroxymonosulfate activation for Rhodamine-B degradation. Chemosphere 228, 412-417.

Patton, S., Li, W., Couch, K.D., Mezyk, S.P., Ishida, K.P., Liu, H., 2016. Impact of the ultraviolet photolysis of monochloramine on 1, 4-dioxane removal: New insights into potable water reuse. Environ. Sci. Technol. Lett. 4, 26-30.

Patton, S., Romano, M., Naddeo, V., Ishida, K.P., Liu, H., 2018. Photolysis of mono-and dichloramines in UV/hydrogen peroxide: Effects on 1, 4-dioxane removal and relevance in water reuse. Environ. Sci. Technol. 52, 11720-11727.

Perrin, D.D., 1972. Dissociation constants of organic bases in aqueous solution: supplement 1972. Butterworths.

Pfaff, F.F., Kundu, S., Risch, M., Pandian, S., Heims, F., Pryjomska-Ray, I., Haack, P., Metzinger, R., Bill, E., Dau, H., Comba, P., Ray, K., 2011. An oxocobalt(IV) complex stabilized by lewis acid interactions with scandium(III) ions. Angew. Chem. Int. Ed. 50, 1711-1715.

Qin, W., Fang, G., Wang, Y., Zhou, D., 2018. Mechanistic understanding of polychlorinated biphenyls degradation by peroxymonosulfate activated with $CuFe_2O_4$ nanoparticles: Key role of superoxide radicals. Chem. Eng. J. 348, 526-534.

Ren, Y., Lin, L., Ma, J., Yang, J., Feng, J., Fan, Z., 2015. Sulfate radicals induced from peroxymonosulfate by magnetic ferrospinel MFe_2O_4 (M = Co, Cu, Mn, and Zn) as heterogeneous catalysts in the water. Appl. Catal., B 165, 572-578.

Ross, A.B., Neta, P., 1979. Rate constants for reactions of inorganic radicals in aqueous solution. US Department of Commerce, National Bureau of Standards Washington D. C.

Rosso, J.A., Allegretti, P.E., Mártire, D.O., Gonzalez, M.C., 1999. Reaction of sulfate and phosphate radicals with α, α, α-trifluorotoluene. J. Chem. Soc. Perkin Trans. 2. 2, 205-210.

Rosso, K.M., Morgan, J.J., 2002. Outer-sphere electron transfer kinetics of metal ion oxidation by molecular oxygen. Geochim. Cosmochim. Acta 66, 4223-4233.

Sekar, R., DiChristina, T.J., 2014. Microbially driven Fenton reaction for degradation of the widespread environmental contaminant 1,4-dioxane. Environ. Sci. Technol. 48, 12858-12867.

Shafirovich, V., Dourandin, A., Huang, W., Geacintov, N.E., 2001. The carbonate radical is a site-selective oxidizing agent of guanine in double-stranded oligonucleotides. J. Biol. Chem. 276, 24621-24626.

Sheng, B., Huang, Y., Wang, Z., Yang, F., Ai, L., Liu, J., 2018. On peroxymonosulfate-based treatment of saline wastewater: when phosphate and chloride co-exist. RSC Adv. 8, 13865-13870.

Son, H.-S., Choi, S.-B., Khan, E., Zoh, K.D., 2006. Removal of 1,4-dioxane from water using sonication: Effect of adding oxidants on the degradation kinetics. Water Res. 40, 692-698.

Wang, Z., Bush, R.T., Sullivan, L.A., Chen, C., Liu, J., 2014. Selective oxidation of arsenite by peroxymonosulfate with high utilization efficiency of oxidant. Environ. Sci. Technol. 48, 3978-3985.

Wardman, P., 1989. Reduction potentials of one-electron couples involving free radicals in aqueous solution. J. Phys. Chem. Ref. Data 18, 1637-1755.

Yang, F., Huang, Y., Fang, C., Xue, Y., Ai, L., Liu, J., Wang, Z., 2018. Peroxymonosulfate/base process in saline wastewater treatment: The fight between alkalinity and chloride ions. Chemosphere 199, 84-88.

Yang, Y., Jiang, J., Lu, X., Ma, J., Liu, Y., 2015. Production of sulfate radical and hydroxyl radical by reaction of ozone with peroxymonosulfate: A novel advanced oxidation process. Environ. Sci. Technol. 49, 7330-7339.

548 Yuan, R., Ramjaun, S.N., Wang, Z., Liu, J., 2011. Effects of chloride ion on degradation of acid orange
549 7 by sulfate radical-based advanced oxidation process: Implications for formation of chlorinated
550 aromatic compounds. J. Hazard. Mater. 196, 173-179.
551 Zhang, Q.Q., Ying, G.G., Pan, C.G., Liu, Y.S., Zhao, J.L., 2015. Comprehensive evaluation of
552 antibiotics emission and fate in the river basins of China: Source analysis, multimedia modeling,
553 and linkage to bacterial resistance. Environ. Sci. Technol. 49, 6772-6782.
554 Zhang, T., Zhu, H., Croué, J.P., 2013. Production of sulfate radical from peroxymonosulfate induced
555 by a magnetically separable $CuFe_2O_4$ spinel in water: Efficiency, stability, and mechanism.
556 Environ. Sci. Technol. 47, 2784-2791.
557 Zhao, L., Hou, H., Fujii, A., Hosomi, M., Li, F., 2014. Degradation of 1, 4-dioxane in water with heat-
558 and Fe^{2+}-activated persulfate oxidation. Environ. Sci. Pollut. Res. 21, 7457-7465.
559 Zhong, H., Brusseau, M.L., Wang, Y., Yan, N., Quig, L., Johnson, G.R., 2015. In-situ activation of
560 persulfate by iron filings and degradation of 1, 4-dioxane. Water Res. 83, 104-111.
561 Zhou, Y., Jiang, J., Gao, Y., Ma, J., Pang, S.Y., Li, J., Lu, X.T., Yuan, L.P., 2015. Activation of
562 peroxymonosulfate by benzoquinone: A novel nonradical oxidation process. Environ. Sci. Technol.
563 49, 12941-12950.
564
565
566

List of Contents in Supporting Information